Measurement xxx (2016) xxx–xxx

Contents lists available at ScienceDirect

Measurement

journal homepage: www.elsevier.com/locate/measurement

Simplified elements for wind-tunnel measurements with type-III-terrain atmospheric boundary layer

Ward De Paepe [a,*], Santiago Pindado [b], Svend Bram [c], Francesco Contino [a]

[a] Vrije Universiteit Brussel, Dept. of Mechanical Engineering (MECH), Pleinlaan 2, 1050 Brussel, Belgium
[b] Universidad Politécnica de Madrid, Instituto Universitario de Microgravedad "Ignacio Da Riva" (IDR/UPM), ETSI Aeronáutica y del Espacio, Pza. Cardenal Cisneros, 3, E-28040 Madrid, Spain
[c] Vrije Universiteit Brussel, Dept. of Industrial Engineering Sciences (INDI), Nijverheidskaai 170, 1070 Brussel, Belgium

ARTICLE INFO

Article history:
Received 9 December 2015
Received in revised form 23 May 2016
Accepted 24 May 2016
Available online xxxx

Keywords:
Atmospheric boundary layer
Hot-wire anemometry
Part-depth ABL wind-tunnel simulation
Truncated vortex generators
Type-III terrain

ABSTRACT

In this work, the results of simulating the ABL over a type III suburban terrain in the industrial wind tunnel of the Department of Mechanical Engineering of the *Vrije Universiteit Brussel* (VUB) are presented. Two different Roughness Barrier Mixing Device (RBMD) methods for simulating the ABL have been used (firstly, the well known combination of Counihan quarter ellipses and roughness elements, and secondly, a new configuration based on truncated Irwin spires and roughness elements). Counihan quarter ellipses are generally considered as the optimal method for ABL simulation. However, its construction is quite complex. Therefore, an alternative setup, using truncated Irwin spires, was experimentally tested. The results of these two simulated ABLs were compared with international standard applicable for type III suburban terrain. Results showed good agreement between standards and experimental results showing that both techniques give a good representation of the ABL. Finally, the proposed truncated Irwin spires method/configuration is confirmed as a proper way to carry out ABL wind tunnel simulations, as the results are practically the same as the ones obtained with the well established Counihan method to simulate ABL in wind tunnels.

© 2016 Published by Elsevier Ltd.

1. Introduction

It is generally accepted that allowing the flow to run over a rough surface producing a natural growth boundary layer is the best method for simulating the Atmospheric Boundary Layer (ABL) in a wind tunnel [1]. Depending on the surroundings of the studied region, a different roughness must be used. When using this technique, the scale of the simulated ABL depends on the length of the roughness fetch. In order to obtain very large scales for the analysis of wind loads on buildings, a specially constructed wind tunnel with a working section that is much longer than its cross sectional dimension is required [2 4]. The formation of this turbulent boundary layer tunnel can be enhanced by using obstructions upstream that have the ability to absorb energy from the mean flow without introducing large scale disturbance [5]. Many different techniques have been studied since 1960, for instance using spires in combination with roughness elements [2,6], air jets [7,8], fences in combination with chains [9] and fences [10] or rods [11]. Finally, a good review of the different techniques to simulate the ABL in a wind tunnel can be found in [12].

The Roughness Barrier Mixing Device (RBMD) method proposed by Cook has simulated successfully the lower third of the boundary layer using turbulence grid, plane barrier wall and roughness elements [13]. These RBMD techniques are renowned for reproducing mean and fluctuating parameters of the atmospheric boundary layer. The RBMD method, suggested by Counihan [14], using elliptic wedge generators in combination with a castellated wall and roughness elements [14 18] allows full depth boundary layer simulations. This method is widely used for full depth ABL simulation [19 25]. An alternative for the RBMD method of Counihan is given by Irwin [26]. Irwin uses the flat triangular spires from Standen et al. [2] as a vortex generator and roughness elements to reproduce full depth boundary layers with a thickness of about 80% of the spire height. The major advantage of the techniques of Irwin [26] compared to the technique of Counihan [14] is the use of triangular spires as vortex generators, the construction of these elements being much easier compared to quarter ellipses. Finally, the use of the flat triangular spires has been referred as Standen method by some authors [27,28].

* Corresponding author.
E-mail address: wdepaepe@vub.ac.be (W. De Paepe).

http://dx.doi.org/10.1016/j.measurement.2016.05.078
0263-2241/© 2016 Published by Elsevier Ltd.

Please cite this article in press as: W. De Paepe et al., Simplified elements for wind tunnel measurements with type III terrain atmospheric boundary layer, Measurement (2016), http://dx.doi.org/10.1016/j.measurement.2016.05.078

UNCORRECTED PROOF

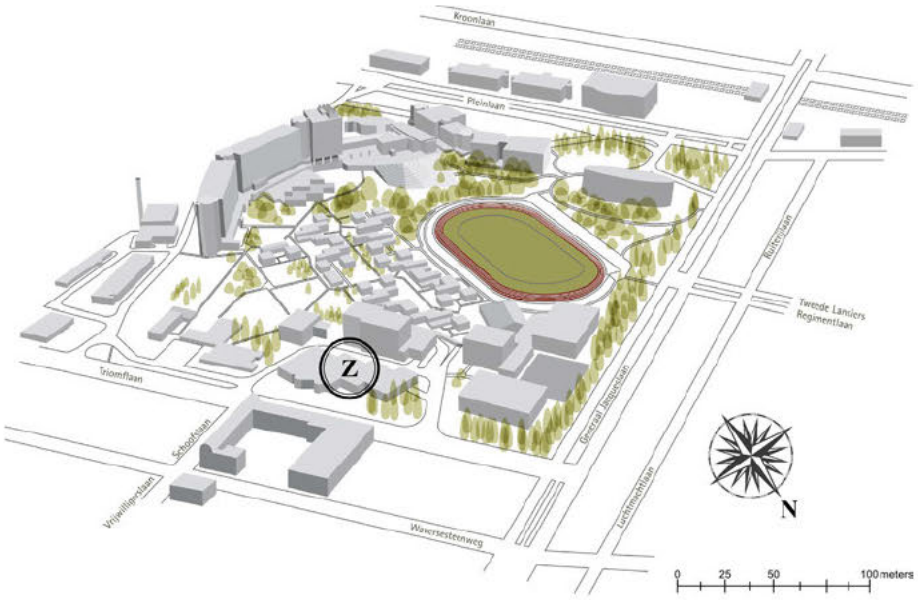

Fig. 1. Suburban terrain at Brussels (Elsene/Ixelles) for which the ABL is simulated. The building Z at the VUB campus is indicated in the image.

Table 1
Main specifications of the industrial wind tunnel at the Mechanical Engineering Department of the VUB.

Type	Open circuit
Total tunnel length	25 m
Testing chamber length	12 m
Testing chamber height	1 m
Testing chamber width	2 m
Turbine power	55 kW
Maximal wind speed	20 m/s

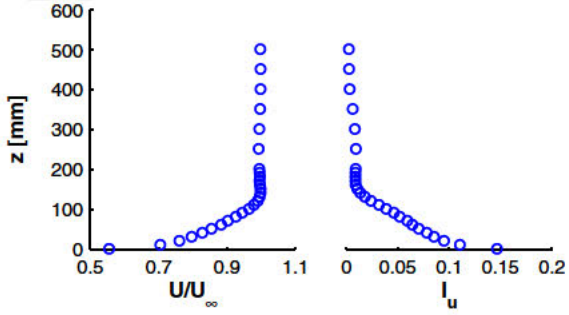

Fig. 2. Flow at testing section of the VUB wind tunnel in clear configuration (i.e., without any ABL simulation).

ABL simulations in a wind tunnel represent a quite complex problem. First of all, the researchers have to deal with the length of the wind tunnel, which normally does not allow for a complete development of the required boundary layer. Therefore, spires and vortex generators need to be installed. Also, the ABL simulations can be performed using full depth simulation or part depth simulation method [13,14,23,26,29,30]. Other problems are the scaling of the Reynolds numbers [31], or the difficulties to simulate the peak suctions on a wind tunnel even with simulated ABL [32], as the conical vortices are incompressible flow structures that perform like a suction amplifier for wind turbulence [33,34]. Besides, once the properly scaled ABL simulation has been achieved for a specific wind tunnel, the results of the wind tunnel testing must be carefully scaled, as they are going to be translated to full scale pressure/forces in a situation where the real boundary layer will never be exactly the same as the one simulated in the wind tunnel. As a consequence, reasonable decisions needs to be taken by researchers when dealing with wind tunnel testing of civil structures, no matter if the facility used is an extremely well equipped one, or a simple facility, even without ABL simulation, is used [35 39].

In the present work, the design and validation of the simulated ABL in the wind tunnel at the VUB are presented. These ABL simulations were developed in order to find a solution to prevent Exhaust Gas Recirculation (EGR) from happening in a micro Gas Turbine (mGT). That research work [40] required simulation of the local ABL at the Elsene/Ixelles municipality of Brussels, this area being a typical example of a suburban terrain in the Benelux. By simulating the ABL in the industrial wind tunnel of the Vrije Universiteit Brussel (VUB), the wind behaviour around the building where the mGT is located (building Z of the VUB campus, see Fig. 1) was analysed (and more in detail around the stack of the mGT). Wind tunnel experiments with a scale model allowed the authors of the study to find a solution for the recurrent problem of EGR, by properly heightening the stack.

The characterising parameters of the ABL are introduced in Section 2 of this study. These parameters have specific values, defined in international standards on turbulent boundary layers, depending on the roughness of the location to be analysed. The definition of each parameter is presented, together with their specific values, for the ABL around aforementioned building Z of the VUB campus. Out of these values, the dimensions of the experimental wind tunnel set up are also determined in Section 2. For the simulations carried out, both Irwin [26] and Counihan [14] RBMD methods were used. In Section 3, the simulated ABLs are validated by measuring and calculating its characteristic parameters and comparing them with the values from the standard codes, in order to select the optimal method to use in wind tunnel simulations. Finally, conclusions are summarised in Section 4.

2. Design of the ABL

The wind tunnel simulations of the ABL were performed in the industrial wind tunnel at the VUB (Table 1). The wind tunnel has a

Please cite this article in press as: W. De Paepe et al., Simplified elements for wind tunnel measurements with type III terrain atmospheric boundary layer, Measurement (2016), http://dx.doi.org/10.1016/j.measurement.2016.05.078

Table 2
Different terrain types specified in the Belgian/European wind standards [45]. Values of the roughness length, z_0, and the atmospheric boundary layer power law exponent, α, according to Dyrbye and Hansen [46] (*) and VDI guideline 3783 [47] (**), have been also included.

Terrain category	z_0 [m]	z_0 (**) [m]	α (*)	α (**)
Type 0. Sea or coastal area exposed to the open sea	0.003	–	–	–
Type I. Lakes or flat and horizontal area with negligible vegetation and without obstacles	0.01	10^{-5}–0.005	0.12	0.08–0.12
Type II. Area with low vegetation such as grass and isolated obstacles (trees, buildings) with separations of at least 20 obstacle heights	0.05	0.005–0.1	0.16	0.18–0.18
Type III. Area with regular cover of vegetation or buildings or with isolated obstacles with separations of maximum 20 obstacle heights (such as villages, suburban terrain, permanent forest)	0.3	0.1–0.5	0.22	0.18–0.24
Type IV. Area in which at least 15% of the surface is covered with buildings and their average height exceeds 15 m	1.0	0.5–2.0	0.30	0.24–0.40

working section of 12 m longitude. The cross section is 2 m wide and 1 m high. The wind velocity can be varied from 0 m/s to 20 m/s by changing the rotations speed of the fan. In the floor of the wind tunnel, a turn table with diameter 2 m is installed to change the approach of the wind on the scale model. The centre of this turn table is located 10 m behind the end of the contraction. The maximum wind speed is 20 m/s, the uniformity of the flow being quite high (160 mm boundary layer thickness, with less than 1% turbulent intensity outside the boundary layer) at the testing section (see Fig. 2).

In the past, wind studies have successfully been performed in this wind tunnel [41,42]. Birinchi, Vanbockryck and Hirsch per formed a wind study on the 'King Baudouin Stadium' (*Koning Bou dewijn Stadion*) [41] and also used this set up to simulate the wind load on the tower of the city hall of Brussels [42].

In following subsections, the characteristics of the ABL over the VUB campus (Fig. 1) are included, the testing setups (roughness/ vortex generators shape and dimensions for the simulation of the ABL) using Irwin and Counihan RBMD methods being also described and discussed. These testing setups do not include any testing model. In case of testing experiments of a suburban config uration, the surroundings of the studied building/structure would have to be reproduced.

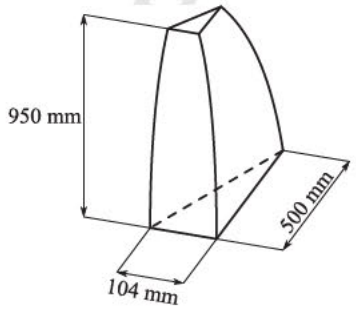

Fig. 3. Dimensions of the elliptic vortex generators.

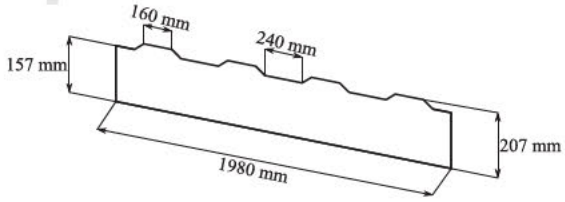

Fig. 4. Design of the castellated barrier wall for ABL simulation in the wind tunnel.

2.1. Properties of the ABL over the VUB campus

The ABL is defined by several parameters. In his review paper, Counihan gives an overview of these parameters [43] and the dif ferent attempts made by researchers to determine experimentally these parameters, for instance by using a captive balloon [44]. These measurements indicated that an inconsistency existed between the parameters defining the ABL, depending on the rough ness of the terrain surrounding the measuring position. By defining from the data four distinct terrain types, these issues could be resolved [43]. The most important parameters for ABL simulation in the wind tunnel are:

- boundary layer height;
- mean velocity profile;
- roughness length;
- intensity of turbulence;
- length scales of turbulence;
- power spectral densities;
- Reynolds stress.

The roughness of the VUB campus surroundings determines the type of boundary layer and the specific value of the different parameters of the ABL. As mentioned by Counihan, four different types of terrain exist [43]: smooth, moderately rough (rural), rough (suburban), very rough (urban). This classification is used in the Belgian/European wind standards [45], with a fifth type terrain added: type 0, very smooth and correspondent to coastal areas exposed to the open sea. See in Table 2 the description of the ter rain types according to the aforementioned standard code (the typ ical values of the roughness length, z_0, and the atmospheric boundary layer power law exponent, α, see Eq. (1) have been also included in the table). For the studied location, the most appropriate, according to the buildings in the neighbourhood, is type III, suburban. This gives the necessary properties of the ABL that should be simulated in the wind tunnel.

Measurements of the ABL showed a boundary layer thickness, δ, depending on the site, of 400 m, up to a maximum of 600 m [43]. Since the maximal height of the wind tunnel at VUB is 1 m, this height was used as boundary layer thickness regarding the first calculations to stablish the ABL simulation set up in the wind tunnel.

The mean wind velocity profile can be determined, as a function of the height over the terrain, z, according to the power law [2]:

$$\frac{U(z)}{U(\delta)} \quad \left(\frac{z}{\delta}\right)^{\alpha} \tag{1}$$

where a suburban wind profile (type III) corresponds to an expo nent of the power law $\alpha = 0.21$ [48]. In this paper, the mean velocity in the x direction U is calculated as

$$U(z) \quad \frac{1}{T}\int_0^T u(z,t)\mathrm{d}t \tag{2}$$

Please cite this article in press as: W. De Paepe et al., Simplified elements for wind tunnel measurements with type III terrain atmospheric boundary layer, Measurement (2016), http://dx.doi.org/10.1016/j.measurement.2016.05.078

When simulating the ABL in the wind tunnel, a shift appears in the profile. This shift is indicated by the zero plane displacement, d. This zero plane displacement will slightly change the power law definition from (1) into

$$\frac{U(z)}{U(\delta)} \quad \left(\frac{z \quad d}{\delta}\right)^{\alpha} \tag{3}$$

Additionally, the roughness length, z_0, of the wind profile is defined as suggested by Thuillier and Lappe [49]:

$$U(z) \quad \frac{u_\tau}{\kappa} \ln\left(\frac{z \quad d}{z_0}\right) \tag{4}$$

where u_τ is the friction velocity, and κ is the von Kármán constant ($\kappa \sim 0.41$). Norms indicate a roughness length $z_0 = 0.3$ m for the suburban region (see Table 2).

The turbulence intensity, I_u, in the x direction can be calculated as follows:

$$I_u(z) \quad \frac{\sigma_u(z)}{U(z)} \quad \frac{\sqrt{\overline{u'^2(z)}}}{U(z)} \tag{5}$$

where

$$u(z,t) \quad U(z) + u'(z,t) \tag{6}$$

and

$$\overline{u'^2(z)} \quad \frac{1}{T}\int_0^T u'^2(z,t)\mathrm{d}t \tag{7}$$

According to Iyengar and Farell, the integral length scale of turbulence, ${}^xL_u$, can be determined in three different ways [50]:

- the value of the spectrum at frequency $f = 0$;
- the area under the autocorrelation curve, $R_{u,x}$, which can be calculated using the following formula

$${}^xL_u \quad \int_0^\infty R_{u,x}(\Delta t)\mathrm{d}t; \tag{8}$$

- the location of the central peak.

Out of the integral length scale of turbulence, the scale of the simulated ABL can be determined using the formula of Cook [51]:

$$S \quad 91.3\frac{(z \quad d)^{0.491}}{{}^xL_u^{1.403} z_0^{0.088}} \tag{9}$$

Both turbulence intensity, I_u, and integral length scale of turbulence, ${}^xL_u$, can be verified, in relation to the height over the terrain, z, using international standards [48,52,53]. It should also be mention that, according to Kozmar, there is a considerable scatter of recommended values for suburban wind characteristics [54].

Finally, the power spectral density of the longitudinal velocity fluctuations at a certain height, $S_u(z,f)$, where

$$\overline{u'^2(z)} \quad \int_0^\infty S_u(z,f)\mathrm{d}f \tag{10}$$

should match a specific profile. Lungu and Gelder pointed out the existence of numerous proposals for the spectral density of along wind gustiness [55]. In this thesis, the profile of the power spectral density will be validated using the formula given by Kaimal et al. [56] for the lower parts, while the ESDU85020 [53], Eurocode1 [48] and von Kármán [57] formulas will be used for the entire thickness of the boundary layer.

The wind velocity in the ABL was only measured in the x direction (see Section 3), making it not possible to calculate the Reynold shear stress

$$\tau \quad \rho\overline{u'w'} \tag{11}$$

In addition, the turbulence intensities, I_v, I_w, and integral length scales, ${}^xL_v$, ${}^xL_w$, of turbulence in y direction and z direction could also not be calculated. Nevertheless, some estimations of these variables can be found in the literature [4]: $I_v \sim 0.75\ I_u$; $I_w \sim 0.5\ I_u$; ${}^xL_v \sim 0.3\ \ 0.4\ {}^xL_u$; and ${}^xL_w \sim 0.5\ \ 0.6\ {}^xL_u$. Besides, it should be also mentioned that quite serious wind tunnel ABL simulation studies, even measuring the three components of the flow velocity, only use as comparison parameters the ones directly related to the x direction of the wind velocity [58].

2.2. Design of truncated Counihan ellipses

A series of test was performed using the method of Counihan [14]. As described by Counihan, the height of the elliptic wedges should be equal to the height of the simulated ABL. For large scales (thus large ABLs), this requires a high wind tunnel cross section. Kozmar suggested the use of truncated elliptic vortex generators instead of the pure Counihan elliptic wedges [59]. After further improving on these techniques, this author was able to perform successfully part depth wind tunnel simulations of the urban [58,60,61], rural and suburban [58] ABL. Analysis of the obtained results indicated the adequacy of redesigned 'Counihan [18]' vortex generators for part depth ABL simulations [58].

Both elliptic vortex generators (Fig. 3) and the castellated barrier wall (Fig. 4), were constructed following Counihan's suggestions [14]. The angle of the elliptic vortex generators is at every height 12° [14], these generators being truncated based on recommendations of Kozmar [58]. The castellated barrier is designed using the properties of the ABL in suburban regions, that is, $\alpha = 0.21$ [48]. For the spacing between the elliptic vortex generators, Counihan suggested a distance of $\delta/2$ [18]. For the placement of the barrier wall, a distance of $\delta/3$ between the barrier wall and the intersect of the working section and the contraction of the wind tunnel, is recommended. Tests of Counihan also suggested a $5\delta/6$ distance between the barrier wall and the elliptic vortex generators [18]. However, the industrial wind tunnel at the VUB is short, so the relative positions of the barrier wall and generators were adapted. For the spacing and the size of the roughness elements, recommendations of Counihan [17], Gartshore and Croos [62] and Fang and Sill [63] were used. As a result, 0.05 m cubes were distributed along the wind tunnel floor. The method described by Gartshore and Croos gives a centre to centre distance for these elements from 27 to 31 cm [62]. For the construction of the surface roughness, polyurethane cubes were attached to a thin wood plate. The Irwin requires a centre to centre distance of 28 cm (see Section 2.3) [26]. To save construction time, for both methods, 28 cm spacing has been used. The complete adapted experimental set up is shown in Fig. 5. Total occupied cross section by the elliptic vortex generators was below 5%. To mitigate a new smoother internal boundary layer growing over the 500 mm between the end of the roughness elements and the turntable, normally roughness elements need to be placed the upstream edge of the turntable. In the specific setup in the wind tunnel of the VUB, this 500 mm is reserved for a scale model of the surroundings, to get accurate simulation of the local surroundings.

2.3. Design of the Irwin spires

A second series of tests was performed using Irwin spires in combination with roughness elements, according to the recommendations of Wooding, Bradley and Marshall [64]. The necessary height of the spires can be calculated, using the formula from Irwin [26]:

$$h \quad \frac{1.39\delta}{1 + \alpha/2} \tag{12}$$

UNCORRECTED PROOF

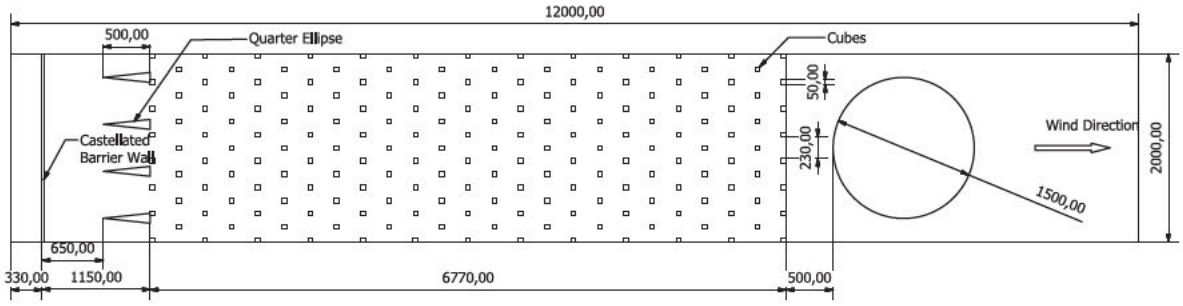

Fig. 5. Arrangement of the truncated vortex generators according to recommendations from Kozmar [58].

Using $\alpha = 0.21$ and $\delta = 1$ m and for Eq. (12) results in a spire height of 1.25 m. The working section of the wind tunnel is how ever only 1 m height. Therefore, it was necessary to truncate the spires at 0.95 m.

The frontal plate base b can be calculated using the formula sug gested by Irwin [26]:

$$\frac{b}{h} \quad 0.5\left[\psi\left(\frac{H}{\delta}(1+\psi)\right)\right]\left(1+\frac{\alpha}{2}\right) \tag{13}$$

with ψ and β from Eq. (13) equal to

$$\psi \quad \frac{\beta\frac{2}{1+\alpha}+\beta \quad \frac{1.13\alpha}{(1+\alpha)(1+\alpha/2)}}{(1 \quad \beta)^2} \tag{14}$$

$$\beta \quad \frac{\delta}{H}\frac{\alpha}{1+\alpha} \tag{15}$$

and H is equal to the height of the wind tunnel.

Irwin suggests that the boundary layer is fully developed after six times the height of the spires [26]. By reducing the skin friction term $1.13\alpha/[(1+\alpha)(1+\alpha/2)]$ from Eq. (14), Lopes, Gomes and Fer reira transformed the formulas for the calculation of the thickness of the spires in order to be able to use Irwin spires in a shorter wind tunnel [65]. Lopes, Gomes and Ferreira suggested a proportional coefficient to the distance reduction of $x/6$. By means of an iterative loop, the optimal positioning of the spires and roughness elements in the tunnel was calculated. The goal was to have at least 50 cm between the scale model and the end of the roughness elements on the tunnel floor, but also to have an optimal use of the total tun nel length. Calculations showed an optimal $x/6$, which results in a frontal plate base $b = 0.182$ m. The separated plate (plate perpen dicular to the base plane, supporting the base to hold the force of the wind) base is 0.314 m, a quarter of the spires height (Fig. 6).

The equations of Irwin for the design of the spires already take into account the existence of roughness elements along the wind tunnel floor [26]. To define the cubes side, k, and the spacing between the cubes, D, the formula of Wooding, Bradley and Mar shall should be used [64]:

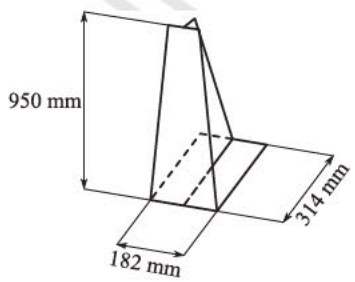

Fig. 6. Dimensions of the truncated Irwin [26] vortex generators.

$$\frac{k}{\delta} \quad \exp\left[\left(\frac{2}{3}\right)\log_{10}\left(\frac{D}{\delta}\right) \quad 0.1161\left[\left(\frac{2}{C_f}\right)+2.05\right]^{0.5}\right] \tag{16}$$

where C_f corresponds to the friction coefficient needed to obtain an α power law velocity profile and is defined as follows:

$$C_f \quad 0.136(\alpha/(1+\alpha))^2 \tag{17}$$

For the 0.05 m side cubes used for the simulations, 0.23 m spac ing between them is necessary.

Spacing between the different spires is equal to $h/2$ from centre line to centre line. Initial tests were carried out using four spires with a centre line distance of 0.5 m. The initial test results how ever showed that the spires were placed too short to each other, resulting in a too high power law exponent ($\alpha = 0.25$). This value corresponds to urban terrain rather than suburban terrain (see Table 2). For the final experiments, three spires were used with a centre line distance of 0.67 m. The final set up used to simulate the ABL in the wind tunnel using Irwin [26] spires is shown in Fig. 7. The blockage ratio obtained with the Irwin method is 15.7%.

3. Characterisation of the simulated ABL

A Dantec Mini Constant Temperature Anemometry (CTA) (accu racy ±1%) of the reading above 5 m/s when calibrated in the wind tunnel with a pitot static tube [66]), with 10 kHz maximal sample rate, was used in the determination of the properties of the ABL. All tests were carried out with a mean free velocity of about 8 m/s. Depending on the application, a different data acquisition rate was used. Used sample rates are specified when discussing the experimental results. The CTA is calibrated using a pitot tube, a four degree calibration curve was fitted to the data. Since no tem perature compensation was foreseen in the calibration, the CTA was calibrated on a daily basis.

3.1. Mean velocity profile

Measurements of the simulated ABL using the truncated ellipses were performed over a measuring period of 20 s, averaged over four periods, using a sample ratio of 10 kHz, while the mea surements using the proposed truncated spires configuration were performed over a larger measuring period of 200 s with a sample ratio of 2.5 kHz. Also, the wind profile corresponding to the trun cated spires configuration was measured with a quite high density of points, that is, with measurements taken every cm. The wind profile regarding the truncated Counihan ellipses configuration was measured with a lower density of points (every 2.5 cm, except the lower part, below 0.25 m, where measurements were taken every cm). The height of the ABL is equal to the height of the tun nel. In the upper part of the ABL, a second boundary layer, due to the ceiling is formed. It is thus not possible to use the free wind velocity as reference for the power law. The reference height is

UNCORRECTED PROOF

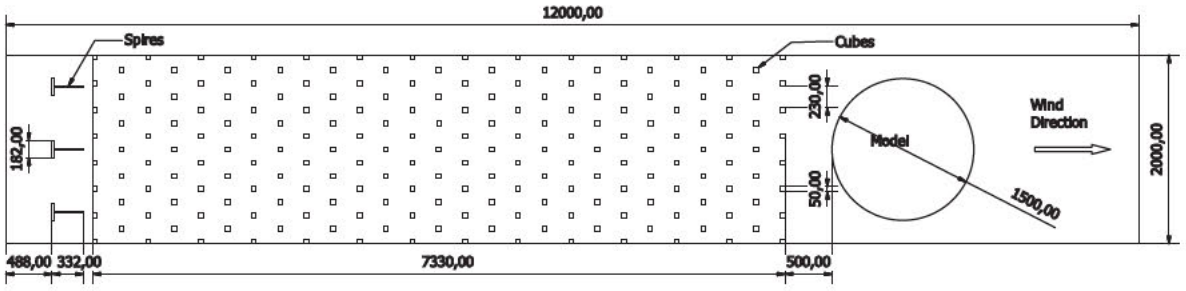

Fig. 7. Arrangement of the vortex generators according to recommendations from Irwin [26].

taken at $z_{ref} = 0.20$ m. This height was arbitrary chosen: high enough to eliminate local effects from the roughness elements and low enough since the ABL is there the strongest. Measurement along the entire wind tunnel height indicated that the effect of the upper boundary layer was noticeable from a height of 0.8 m. Therefore, all measurements above 0.8 m were discarded.

Both methods show good accordance with the power law profile in the lower part of the wind tunnel (Figs. 8 and 9). For the upper part of the simulated ABL, it is clear to see that the profile simulated using truncated Irwin [26] spires keeps following the power law, while measurements with the truncated ellipses of Kozmar [58] start to divert from the profile at a certain height, around $z = 0.28$ m. From this height results indicate a more linear behaviour of the average wind speed. This indicates that not enough vorticity is introduced in the boundary layer due to a too low energy absorption by the ellipses.

It should also be mentioned that, to achieve the power law exponent, Eq. (1) needed to be modified, since u_δ is not known. Modifying the power law results in the formula given by Wang et al. [67]:

$$\frac{u}{u_{ref}} \quad \left(\frac{z \quad d}{z_{ref} \quad d}\right)^{\alpha} \tag{18}$$

Fitting the above equation to the measurements, indicated a power law exponent for both methods of $\alpha = 0.21$ and a displacement height of $d = 15$ mm for the Irwin method and $d = 1$ mm using the truncated ellipses from Kozmar. As aforementioned, a power law exponent of $\alpha = 0.21$ corresponds to suburban wind profiles (type III terrain, see Table 2). Within this curve fit, both power law exponent α and displacement height d were obtained simultaneous.

On the other hand, fitting the profiles to the logarithmic law allows the determination of the roughness length z_0 (Figs. 10 and 11), resulting in $z_0 = 1.2$ mm for the Irwin method and $z_0 = 1.4$ mm for the Kozmar method. When using the scales calculated from the integral length scale (see Section 3.3), full scale

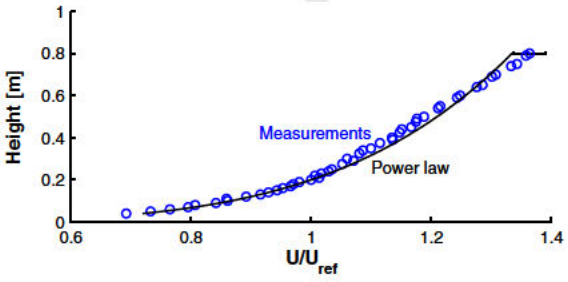

Fig. 8. Simulations of the ABL using truncated Counihan [14] ellipses in combination with roughness elements. Curve fitting indicates a power law exponent $\alpha = 0.21$, and coefficient of determination $R^2 = 0.9898$.

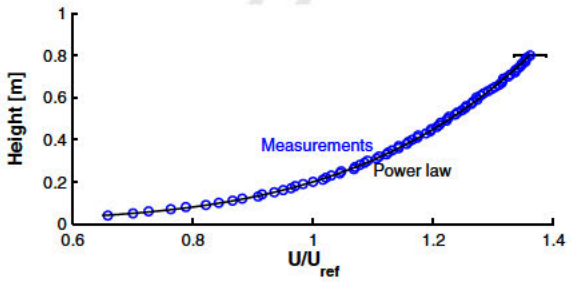

Fig. 9. Simulations of the ABL using truncated Irwin [26] spires in combinations with roughness elements. Curve fitting indicates a power law exponent $\alpha = 0.21$, and coefficient of determination $R^2 = 0.9995$.

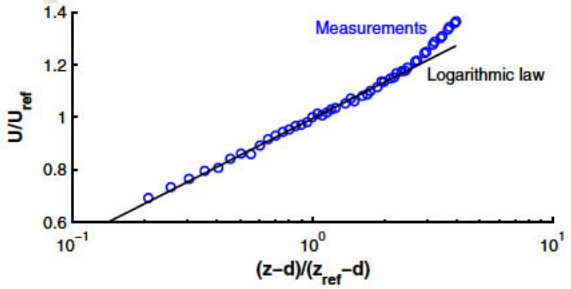

Fig. 10. ABL simulation using truncated Counihan [14] ellipses in combination with roughness elements. Non-dimensional wind speed, U/U_{ref}, as a function of the height over the wind tunnel floor, z, related to the reference height, z_{ref}, (taking also into account the displacement height, d).

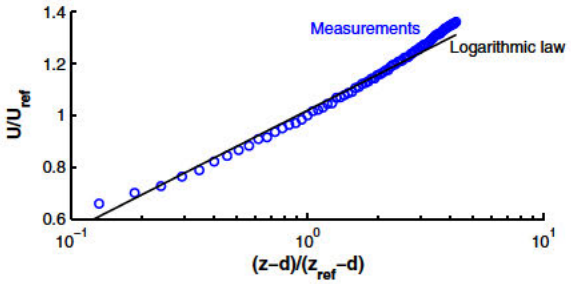

Fig. 11. ABL simulation using truncated Irwin [26] spires in combinations with roughness elements. Non-dimensional wind speed, U/U_{ref}, as a function of the height over the wind tunnel floor, z, related to the reference height, z_{ref}, (taking also into account the displacement height, d).

roughness length for both methods are 0.43 m and 0.55 m, which is close to the 0.3 m given in the Eurocode1 for the suburban terrain category (see Table 2). The friction velocity u_τ in both cases is equal to 0.526 m/s and 0.554 m/s respectively. Both profiles

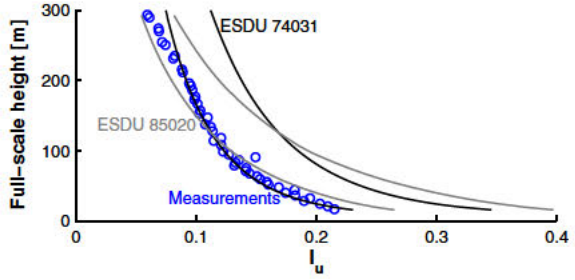

Fig. 12. ABL simulation using truncated Counihan [14] quarter ellipses in combinations with roughness elements. Turbulence intensity, I_u, as a function of the full-scale height (scale of 1:390 was used, scale calculation is based on turbulence length scale calculations). Data compared to results from ESDU74031 [52] and ESDU8502 [53].

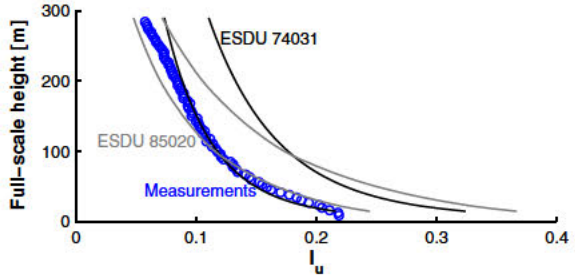

Fig. 13. ABL simulation using truncated Irwin [26] spires in combination with roughness elements. Turbulence intensity, I_u, as a function of the full-scale height (scale of 1.363 was used, scale calculation is based on turbulence length scale calculations). Data compared to results from ESDU74031 [52] and ESDU8502 [53].

show good accordance to the logarithmic law for the lower part of the simulated boundary layer, as was indicated in literature [13]. For higher values, the measurements start to diverge from the log arithmic law, as it was indicated by Cook [13], since the logarith mic law is only valid in the lower part of the ABL. Similar to the curve fit with the power low, for the log law curve fit, again both roughness length z_0 and friction velocity u_τ were obtained simulta neous. For the value of the displacement height d, the value obtained in the power low curve fit was used.

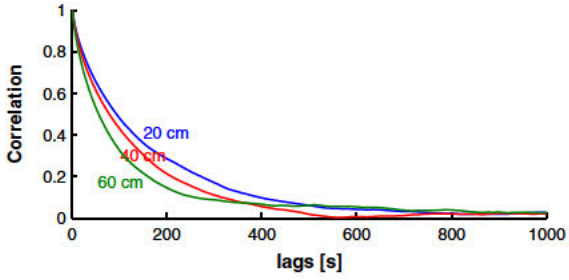

Fig. 15. Autocorrelation curve of velocity measurements at different heights (20, 40 and 60 cm), corresponding to the truncated Irwin spires configuration wind profile.

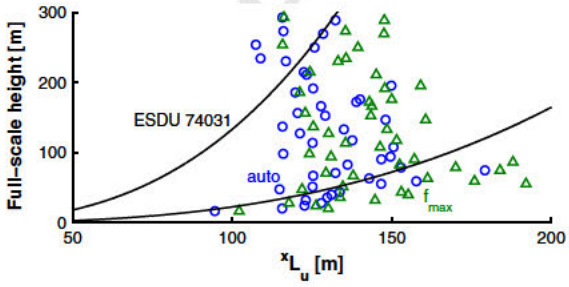

Fig. 16. ABL simulation using truncated Counihan [14] quarter ellipses in combinations with roughness elements. Integral turbulence length scale, ^xL_u, as a function of the full-scale height. Data from ESDU74031 has been added. Blue circles indicate scales calculate with the area under the autocorrelation curve (Method II in the text, "auto" in the figure); green triangles indicate scales calculated based on the location of the central peak (Method III in the text, "f_{max}" in the figure). (For interpretation of the references to colour in this figure legend, the reader is referred to the web version of this article.)

3.2. Turbulence profile

As said in Section 2.1, next to the correct average wind speed profile it is necessary to produce a correct turbulence intensity pro file in order to perform a correct ABL simulation. Using the mea surements taken for the velocity profile, the turbulence intensity I_u was calculated in both studied cases, see Figs. 12 and 13. These results are compared with turbulence intensity data from ESDU74031 and ESDU85020 international codes [52,53], for the corresponding roughness of the terrain. In both standards, the tur bulence profile is defined within two boundaries.

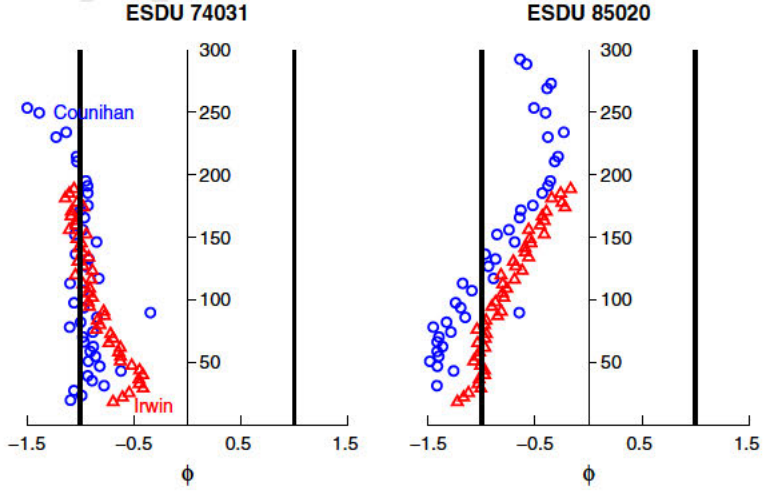

Fig. 14. Difference between the measured turbulence profiles and data from ESDU74031 [52] and ESDU85020 [53], analysed with variable ϕ, defined in Eq. (19).

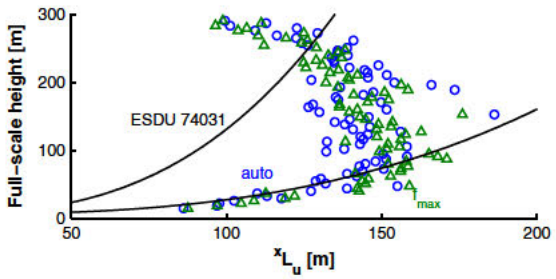

Fig. 17. ABL simulation using truncated Irwin [26] spires in combination with roughness elements. Integral turbulence length scale, $^{x}L_u$, as a function of the full-scale height. Data from ESDU74031 has been added. Blue circles indicate scales calculate with the area under the autocorrelation curve (Method II in the text, "auto" in the figure); green triangles indicate scales calculated based on the location of the central peak (Method III in the text, "f_{max}" in the figure). (For interpretation of the references to colour in this figure legend, the reader is referred to the web version of this article.)

For the comparison with ESDU74031 and ESDU85020 standards, the measurement data was scaled to actual height. The scaling factor obtained for the Counihan method is 1:390, while a scale of 1:363 was obtained for the Irwin method. These scaling factors were calculated from the measurement data. More details about the scale determination are included in the following subsection. Both measurement data from Figs. 12 and 13 show good correspondence to the standards. Both profiles follow the given trend. However, results are close to the lower boundary defined in the aforementioned standards, indicating that a minimum of turbulence is introduced in the simulated boundary layer.

In order to compare more precisely the results from both configurations studied the following variable has been defined:

$$\phi \quad \frac{I_u \quad I_{u,ESDU}}{0.2 \cdot I_{u,\mathrm{ESDU}}} \tag{19}$$

where I_u is the measured turbulence intensity, and $I_{u,\mathrm{ESDU}}$ is the turbulent intensity defined in the ESDU standard. Obviously, if the measured turbulence profile is between the upper and lower limits of the ESDU standards data from Figs. 12 and 13, the value of ϕ will be in the bracket [1,1]. In Fig. 14 the values of ϕ, calculated for both ESDU74031 and ESDU85020 data are plotted as a function of the full scale height. It is quite clear from Fig. 14 that results obtained with the configuration based on the proposed truncated Irwin spires, are closer to the data from the aforementioned ESDU standards.

3.3. Integral length scale of turbulence

The integral length scale of turbulence is important to determine the final length scale of the simulated ABL. As previously mentioned, the integral length scale of turbulence, $^{x}L_u$, can be determined in three different ways: Method I: the value of the spectrum at frequency $f = 0$; Method II: the area under the autocorrelation curve; and Method III: the location of the central peak.

According to Iyengar and Farell, the errors involved in the determination of the sample spectral values at $f = 0$ (Method I) are quite

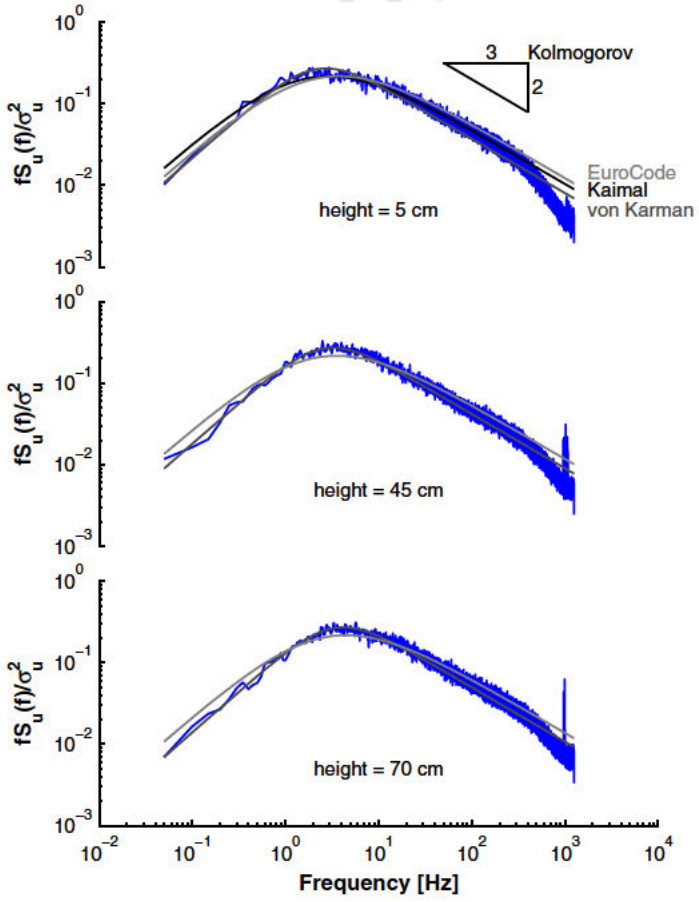

Fig. 18. ABL simulation using truncated Counihan [14] quarter ellipses in combinations with roughness elements. Power spectral density measured at three different heights. Kaimal et al. [56], Eurocode 1 [48] and Von Kármán spectrums [57] and the Kolmogorov −2/3 slope [69] have been included in the graphs.

Please cite this article in press as: W. De Paepe et al., Simplified elements for wind tunnel measurements with type III terrain atmospheric boundary layer, Measurement (2016), http://dx.doi.org/10.1016/j.measurement.2016.05.078

significant unless one has adequate resolution and definition of the spectra at low frequencies [50]. In their work, these authors measured the velocity fluctuations over three intervals of 2, 0.2 and 0.05 ms with inline low pass filters set at frequencies of 0.2, 1 and 5 kHz. Such filters were not available. Therefore, the integral length scale of turbulence was calculated using Methods II and III.

The autocorrelation curve (Method II) and the location of the central peak (method III) were obtained using Matlab®. The measurement intervals were split in different additional intervals of 2 s, using a Hamming window. The final autocorrelation was calculated using the *pwelch* function [68]. Ideally, the integral turbulence length scales are calculated taking the complete surface under the autocorrelation curve. This means taking the integral between limits zero and infinity (Eq. (10)). However, since velocity was measured over a finite period, the autocorrelation curve was cut off after 1000 samples, given that it seemed to be sufficiently converged (see in Fig. 15 the autocorrelation curve of velocity measurements taken at three different heights of the wind profile corresponding to the truncated Irwin spires configuration). Regarding Method III, rather than directly taking the central frequency, which introduces errors due to the noise, the frequency was determined by fitting the data to the von Kármán spectrum [57]. This allowed for a more correct determination of the maximum frequency.

The integral lengths scale profiles of the simulated ABL using the analysed Counihan and truncated Irwin spires configurations correspond with each other (Figs. 16 and 17). The simulation results agree moderately with the ESDU74031 data, even when taking into account the 30% spread on the standard data. The experimental results are not compared with ESDU85020 data, since Kozmar indicated that the recommended turbulence length scales are much larger in the ESDU85020 standards, compared to other standards [54]. A linear increase of the turbulence integral length scales with height, similar to full scale results, is however not observed. Experimental results increase strong in the near ground region, but with further increase in height, the turbulence length scale remains nearly constant. This trend was reported in other wind tunnel studies as well [50,54]. The different mechanisms of boundary layer development in wind tunnel simulations and in full scale is indicated as a possible explanation by Kozmar [60].

Integral length scales from Figs. 16 and 17 are shown on full scale using the same scales as for Figs. 12 and 13 (1:390 and 1:363). These scales were obtained by using Eq. (9) to calculate the scale [51], using the integral length scales from Figs. 16 and 17. Since the results of the integral length scales show some significant variation, rather than calculating the scale for one single value (at 0.20 m height), as final scale value, an average value over an interval around this reference height was taken to reduce the effect of this variation.

3.4. Power spectral density

For the comparison with the wind power spectral density, several formulas are formulated by different authors in literature [45,53,56,57].

Close to the surface, the power spectral density should correspond to the Kaimal spectrum [56]:

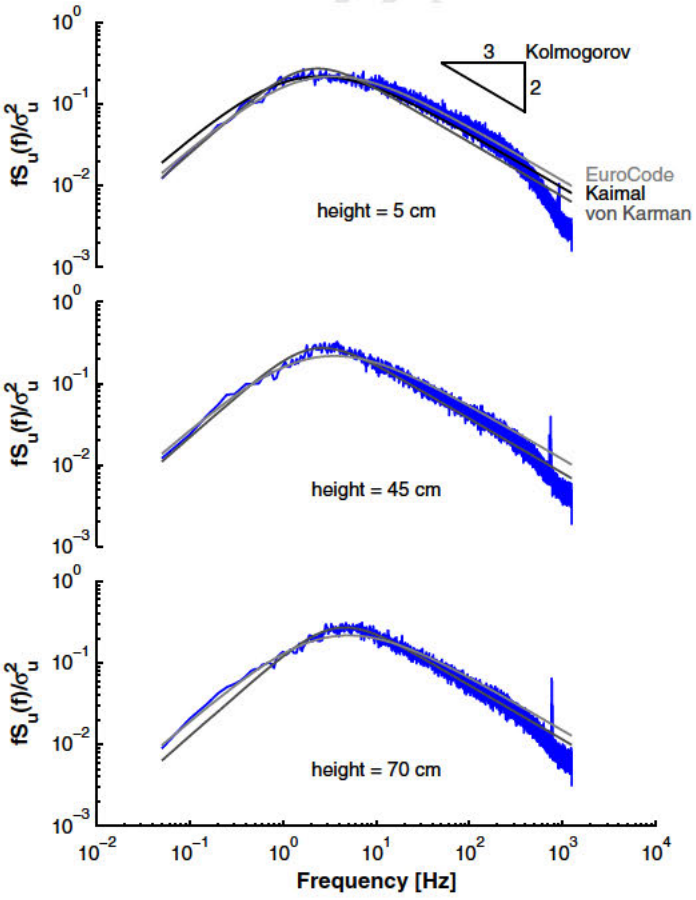

Fig. 19. ABL simulation using truncated Irwin [26] spires in combination with roughness elements. Power spectral density measured at three different heights. Kaimal et al. [56], Eurocode 1 [48] and Von Kármán spectrums [57] and the Kolmogorov −2/3 slope [69] have been included in the graphs.

Please cite this article in press as: W. De Paepe et al., Simplified elements for wind tunnel measurements with type III terrain atmospheric boundary layer, Measurement (2016), http://dx.doi.org/10.1016/j.measurement.2016.05.078

$$\frac{fS_u(f)}{\sigma_u^2} \quad \frac{6.8f_L}{3(1+50f_L)^{5/3}} \tag{20}$$

where f_L, the reduced frequency, is defined as $fz/\bar{u}$.

The Kaimal spectrum gives a good approximation of the power spectral density, up to 50 m [56]. For heights above 50 m, it is more appropriate to compare the power spectral density curve with the spectrum given in Eurocode1 [45]:

$$\frac{fS_u(f)}{\sigma_u^2} \quad \frac{6.8f_L}{\left(1+10.2f_L^2\right)^{5/3}} \tag{21}$$

where f_L $f^xL_u/\bar{u}$. This spectrum is similar to the von Kármán spectrum [57]:

$$\frac{fS_u(f)}{\sigma_u^2} \quad \frac{4f_L}{\left(1+70.8f_L^2\right)^{5/6}} \tag{22}$$

The ESDU74031 standard proposes the von Kármán spectrum to be used to match the power spectral density [53], while ESDU85020 proposes the use of the theoretical model of Kol mogorov [69], where the power spectral density follows a 2/3 slope in the inertial subrange.

Power spectral density results regarding both studied ABL sim ulation methods (Figs. 18 and 19) show good correspondence to the norms close the ground [56] and over the entire boundary layer [45,52,53]. For the determination of the power spectral density of the two simulation methods (truncated Irwin spires and truncated Counihan ellipses) at different heights of 5, 45 and 70 cm, addi tional measurements were performed. For each simulation method and at each different height, 10 additional time series of 200 s, using a sample frequency of 2.5 kHz were recorded and processed. The power spectral densities show maxima between frequencies of 2 and 10 Hz and they follow the Kolmogorov 2/3 slope [69] in the inertial subrange indicating a similar path in turbulent boundary layer structure not dependent on the simulation length scale. With increasing height, the power spectral density maximum shifts to higher frequency. For both analysed ABL simulation methods and the different height, the power spectra die off at the same frequency.

4. Conclusions

In the present work two different wind tunnel ABL simulations are compared. The full scaled ABL was identified as suburban (ter rain type III). The ABL was simulated in the wind tunnel using two simulations techniques: truncated Counihan ellipses in combina tion with a castellated barrier wall and roughness elements, and truncated Irwin spires in combination with roughness elements. Despite the limitations of measuring only the x direction of the wind velocity, the different characteristics of the simulated ABLs showed good correspondence to data from international standards. These ABLs are enough to performed quite accurate wind load analysis on buildings if the proper scaling of the mock up is achieved. However, if more sophisticated testing is planned (i.e., smoke diffusion) checking of the proper vertical and lateral turbulence levels would be required ($I_v \sim 0.75\ I_u$; $I_w \sim 0.5\ I_u$; ${}^xL_v \sim 0.3\ 0.4\ {}^xL_u$; and ${}^xL_w \sim 0.5\ 0.6\ {}^xL_u$), together with the hori zontal pressure gradient compensation.

Both analysed methods showed to be able to simulate a repre sentative boundary layer with scales of around 1:390 (Counihan method) and 1:363 (Irwin method). The ABL simulated with the truncated Irwin spires showed slightly better results than the ones from the truncated Counihan spires, when compared to velocity and turbulence intensity profiles from the standard codes of prac tice. Therefore, it can be said that the more simple method to develop the wind tunnel ABL simulation seems to be a good, quick and inexpensive solution. Besides, the testing configuration setups might be a starting point for other researchers when doing wind tunnel testing with ABL simulation.

Acknowledgements

The research was funded by the National Fund for Scientific Research (FWO). Authors are grateful to the Reviewers, whose wise comments helped to improve this work.

References

[1] M. Jensen, N. Franck, Model-Scale Tests in Turbulent Wind: Part I, Phenomena Dependent on the Wind Speed: Shelter at Houses-Dispersal of Smoke, The Danish Technical Press, Copenhagen, 1963.
[2] N.M. Standen, W.A. Dalgliesh, R.J. Templin, A Wind Tunnel and Full-Scale Study of Turbulent Wind Pressures on a Tall Building, National Research Council, Canada, 1971.
[3] K.A. de Croos, Wind Tunnel Simulations of the Atmospheric Boundary Layer, University of Notre Dame, 1974.
[4] W.H. Snyder, Guideline for Fluid Modeling of Atmospheric Diffusion, Environmental Sciences Research Laboratory, Office of Research and Development, US Environmental Protection Agency, 1981.
[5] T.V. Lawson, Methods of producing velocity profiles in wind tunnels, Atmos. Environ. 2 (1968) 73–76.
[6] W.D. Lubitz, B.R. White, Atmospheric boundary layer wind tunnel applications in wind turbine siting, in: Proceedings of world wind energy conference, 2004.
[7] J.P. Schon, P. Mery, A preliminary study of the simulation of neutral atmospheric boundary layer using air injection in a wind tunnel, Atmos. Environ. 5 (1971) (1967) 299–311.
[8] T.J. Sluman, H.R.E. van Maanen, G. Ooms, Atmospheric boundary layer simulation in a wind tunnel, using air injection, Appl. Sci. Res. 36 (1980) 289–307.
[9] Y. Ohya, Wind-tunnel study of atmospheric stable boundary layers over a rough surface, Bound.-Layer Meteorol. 98 (2001) 57–82.
[10] A.J. Bowen, D. Lindley, A wind-tunnel investigation of the wind speed and turbulence characteristics close to the ground over various escarpment shapes, Bound.-Layer Meteorol. 12 (1977) 259–271.
[11] P.H.A. Barbosa, M. Cataldi, A.P.S. Freire, Wind tunnel simulation of atmospheric boundary layer flows, J. Braz. Soc. Mech. Sci. 24 (2002) 177–185.
[12] A.M. Aly, Atmospheric boundary-layer simulation for the built environment: past, present and future, Build. Environ. 75 (2014) 206–221.
[13] N.J. Cook, On simulating the lower third of the urban adiabatic boundary layer in a wind tunnel, Atmos. Environ. 7 (1973) 691–705.
[14] J. Counihan, An improved method of simulating an atmospheric boundary layer in a wind tunnel, Atmos. Environ. 3 (1969) 197–214.
[15] J. Armitt, J. Counihan, The simulation of the atmospheric boundary layer in a wind tunnel, Atmos. Environ. 2 (1968) 49–71.
[16] J. Counihan, Further measurements in a simulated atmospheric boundary layer, Atmos. Environ. 4 (1970) 259–275.
[17] J. Counihan, Wind tunnel determination of the roughness length as a function of the fetch and the roughness density of three-dimensional roughness elements, Atmos. Environ. 5 (1971) 637–642.
[18] J. Counihan, Simulation of an adiabatic urban boundary layer in a wind tunnel, Atmos. Environ. 7 (1973) 673–689.
[19] S. Rafailidis, Influence of building areal density and roof shape on the wind characteristics above a town, Bound.-Layer Meteorol. 85 (1997) 255–271.
[20] C. Farell, A.K.S. Iyengar, Experiments on the wind tunnel simulation of atmospheric boundary layers, J. Wind Eng. Ind. Aerodyn. 79 (1999) 11–35.
[21] M. Gu, Y. Quan, Across-wind loads of typical tall buildings, J. Wind Eng. Ind. Aerodyn. 92 (2004) 1147–1165.
[22] T. Balendra, D.A. Shah, K.L. Tey, S.K. Kong, Evaluation of flow characteristics in the NUS-HDB Wind Tunnel, J. Wind Eng. Ind. Aerodyn. 90 (2002) 675–688.
[23] M.E. De Bortoli, B. Natalini, M.J. Paluch, M.B. Natalini, Part-depth wind tunnel simulations of the atmospheric boundary layer, J. Wind Eng. Ind. Aerodyn. 90 (2002) 281–291.
[24] N. Kiyoyuki, Wind tunnel modeling of hourly observed atmospheric diffusion by oscillating blade cascade, J. Wind Eng. Ind. Aerodyn. 93 (2005) 99–113.
[25] J.S. Rodrigo, J. van Beeck, G. Dezsö-Weidinger, Wind tunnel simulation of the wind conditions inside bidimensional forest clear-cuts. Application to wind turbine siting, J. Wind Eng. Ind. Aerodyn. 95 (2007) 609–634.
[26] H.P.A.H. Irwin, The design of spires for wind simulation, J. Wind Eng. Ind. Aerodyn. 7 (1981) 361–366.
[27] A.R. Wittwer, S.V. Möller, Characteristics of the low-speed wind tunnel of the UNNE, J. Wind Eng. Ind. Aerodyn. 84 (2000) 307–320.
[28] A. Poitevin, B. Natalini, L.A. Godoy, Pressures on open canopy structures with parapets under wind loading, Eng. Struct. 56 (2013) 850–867.
[29] N.J. Cook, Wind-tunnel simulation of the adiabatic atmospheric boundary layer by roughness, barrier and mixing-device methods, J. Wind Eng. Ind. Aerodyn. 3 (1978) 157–176.

UNCORRECTED PROOF

[30] E. Torres García, M. Ogueta-Gutiérrez, S. Ávila, S. Franchini, E. Herrera, J. Meseguer, On the effects of windbreaks on the aerodynamic loads over parabolic solar troughs, Appl. Energy 115 (2014) 293–300.
[31] P.A. Irwin, Wind engineering research needs, building codes and project specific studies, in: Proceedings of the 11th Americas Conference on Wind Engineering, 2009.
[32] E. Simiu, Wind loading codification in the Americas: fundamentals for a renewal, in: Proceedings of the 11th Americas Conference on Wind Engineering, San Juan, Puerto Rico, USA, 2009.
[33] D. Banks, R. Meroney, A model of roof-top surface pressures produced by conical vortices: model development, Wind Struct. 4 (2001) 227–246.
[34] D. Banks, R. Meroney, A model of roof-top surface pressures produced by conical vortices: evaluation and implications, Wind Struct. 4 (2001) 279–298.
[35] S. Pindado, J. Meseguer, Wind tunnel study on the influence of different parapets on the roof pressure distribution of low-rise buildings, J. Wind Eng. Ind. Aerodyn. 91 (2003) 1133–1139.
[36] S. Pindado, J. Meseguer, S. Franchini, The influence of the section shape of box-girder decks on the steady aerodynamic yawing moment of double cantilever bridges under construction, J. Wind Eng. Ind. Aerodyn. 93 (2005) 547–555.
[37] S. Franchini, S. Pindado, J. Meseguer, A. Sanz-Andrés, A parametric, experimental analysis of conical vortices on curved roofs of low-rise buildings, J. Wind Eng. Ind. Aerodyn. 93 (2005) 639–650.
[38] S. Pindado, J. Meseguer, S. Franchini, Influence of an upstream building on the wind-induced mean suction on the flat roof of a low-rise building, J. Wind Eng. Ind. Aerodyn. 99 (2011) 889–893.
[39] J. Meseguer, A. Sanz Andrés, S. Pindado, S. Franchini, G. Alonso, Aerodinámica Civil 2ª Edición. Efectos del viento en edificaciones y estructuras, Ibergarceta Publicaciones, S.L., 2013.
[40] W. De Paepe, F. Delattin, S. Bram, J. De Ruyck, Discussion of the effects of recirculating exhaust air on performance and efficiency of a typical microturbine, Energy 45 (2012) 456–463.
[41] H. Birinchi, H. Vanbockryck, C. Hirsch, Windtunnelstudie van het stromingspatroon in het koning boudewijn stadion, Vrije Universiteit Brussel, Pleinlaan 2, 1050 Brussel, 1996.
[42] R. Derdelinckx, C. Hirsch, Windtunnelstudie van het stadhuis te Brussel, Vrije Universitiet Brussel, Pleinlaan 2, 1050 Brussel, 1993.
[43] J. Counihan, Adiabatic atmospheric boundary layers: a review and analysis of data from the period 1880–1972, Atmos. Environ. 9 (1975) 871–905.
[44] P.M. Jones, M.A.B. de Larrinaga, C.B. Wilson, The urban wind velocity profile, Atmos. Environ. 5 (1971) 89–90. IN81–IN83, 91–102.
[45] Belgisch instituut voor normalisatie (BIN), Eurocode1: Belastingen op constructies – Deel 1–4: Algemene belastingen – Windbelasting, 2005.
[46] C. Dyrbye, S.O. Hansen, Wind Loads on Structures, 1997.
[47] VDI Guideline 3783, Part 1: Dispersion of Pullutants in the Atmosphere; Dispersion of Emissions by Accidental Releases; Safety Study, Issue: 07/1990, 1987.
[48] Belgisch instituut voor normalisatie (BIN), Eurocode1: Actions on Structures. Wind Actions, 2002.
[49] R.H. Thuillier, U.O. Lappe, Wind and temperature profile characteristics from observations on a 1400 ft tower, J. Appl. Meteorol. 3 (1964) 299–306.
[50] A.K.S. Iyengar, C. Farell, Experimental issues in atmospheric boundary layer simulations: roughness length and integral length scale determination, J. Wind Eng. Ind. Aerodyn. 89 (2001) 1059–1080.
[51] N.J. Cook, Determination of the model scale factor in wind-tunnel simulations of the adiabatic atmospheric boundary layer, J. Wind Eng. Ind. Aerodyn. 2 (1978) 311–321.
[52] Engineering Sciences Data Unit (ESDU), Characteristics of Atmospheric Turbulence Near the Ground, Part II: Single Point Data for Strong Winds (Neutral Atmosphere), 1974.
[53] Engineering Sciences Data Unit (ESDU), Characteristics of Atmospheric Turbulence Near the Ground, Part II: Single Point Data for Strong Winds (Neutral Atmosphere), 1985.
[54] H. Kozmar, Wind-tunnel simulations of the suburban ABL and comparison with international standards, Wind Struct. 14 (2011) 15–34.
[55] D. Lungu, P.V. Gelder, Characteristics of Wind Turbulence with Applications to Wind Codes, ESREL 2003 (European Safety and Reliability Conference), 2003, pp. 1271–1277.
[56] J.C. Kaimal, J.C. Wyngaard, Y. Izumi, O.R. Cote, Spectral characteristics of surface-layer turbulence, Quart. J. Roy. Meteorol. Soc. 98 (1972) 563–589.
[57] T. von Kármán, Progress in the statistical theory of turbulence, Proc. Natl. Acad. Sci. U.S.A. 34 (1948) 530–539.
[58] H. Kozmar, Truncated vortex generators for part-depth wind-tunnel simulations of the atmospheric boundary layer flow, J. Wind Eng. Ind. Aerodyn. 99 (2011) 130–136.
[59] H. Kozmar, Natural wind simulation in the TUM boundary layer wind tunnel, in: C. Borri (Ed.), 5th European & African Conference on Wind Engineering, Florence, Italy, 2009.
[60] H. Kozmar, Scale effects in wind tunnel modeling of an urban atmospheric boundary layer, Theor. Appl. Climatol. 100 (2010) 153–162.
[61] H. Kozmar, An alternative approach to experimental simulation of wind characteristics in urban environments, Proc. Environ. Sci. 4 (2011) 43–50.
[62] I.S. Gartshore, K.A.D. Croos, Roughness element geometry required for wind tunnel simulations of the atmospheric wind, J. Fluids Eng. 99 (1977) 480–485.
[63] C. Fang, B.L. Sill, Aerodynamic roughness length: correlation with roughness elements, J. Wind Eng. Ind. Aerodyn. 41 (1992) 449–460.
[64] R.A. Wooding, E.F. Bradley, J.K. Marshall, Drag due to regular arrays of roughness elements of varying geometry, Bound.-Layer Meteorol. 5 (1972) 285–308.
[65] M.F.P. Lopes, M.G. Gomes, J.G. Ferreira, Simulation of the atmospheric boundary layer for model testing in a short wind tunnel, Exp. Tech. 32 (2008). 1747-1567.
[66] F.E. Jørgensen, How to measure turbulence with hot-wire anemometers — a practical guide. in: D. Dunamics (Ed.), Skovlunde, Denmark, 2002. <http://www.dantecdynamics.com/how-to-measure-turbulence-practical-guide> (accessed: 9-09-2014).
[67] Z.Y. Wang, E.J. Plate, M. Rau, R. Keiser, Scale effects in wind tunnel modelling, J. Wind Eng. Ind. Aerodyn. 61 (1996) 113–130.
[68] G. Heinzel, A. Rüdiger, R. Schilling, T. Hannover, Spectrum and spectral density estimation by the Discrete Fourier transform (DFT), including a comprehensive list of window functions and some new flat-top windows, Max Plank Inst. 12 (2002) 122.
[69] A.N. Kolmogorov, The local structure of turbulence in incompressible viscous fluid for very large Reynolds numbers, in: Dokl. Akad. Nauk SSSR, 1941, pp. 299–303.

UNCORRECTED PROOF

Please cite this article in press as: W. De Paepe et al., Simplified elements for wind tunnel measurements with type III terrain atmospheric boundary layer, Measurement (2016), http://dx.doi.org/10.1016/j.measurement.2016.05.078